REFERENCES

1. Suda, T., Takubo, K., and Semenza, G. L. (2011) Metabolic regulation of hematopoietic stem cells in the hypoxic niche. *Cell Stem Cell* **9**, 298-310
2. Levesque, J. P., Helwani, F. M., and Winkler, I. G. (2010) The endosteal 'osteoblastic' niche and its role in hematopoietic stem cell homing and mobilization. *Leukemia* **24**, 1979-1992
3. Chow, D. C., Wenning, L. A., Miller, W. M., and Papoutsakis, E. T. (2001) Modeling pO(2) distributions in the bone marrow hematopoietic compartment. II. Modified Kroghian models. *Biophys J* **81**, 685-696
4. Calvi, L. M., Adams, G. B., Weibrecht, K. W., Weber, J. M., Olson, D. P., Knight, M. C., Martin, R. P., Schipani, E., Divieti, P., Bringhurst, F. R., Milner, L. A., Kronenberg, H. M., and Scadden, D. T. (2003) Osteoblastic cells regulate the haematopoietic stem cell niche. *Nature* **425**, 841-846
5. Zhang, J., Niu, C., Ye, L., Huang, H., He, X., Tong, W. G., Ross, J., Haug, J., Johnson, T., Feng, J. Q., Harris, S., Wiedemann, L. M., Mishina, Y., and Li, L. (2003) Identification of the haematopoietic stem cell niche and control of the niche size. *Nature* **425**, 836-841
6. Arai, F., Hirao, A., Ohmura, M., Sato, H., Matsuoka, S., Takubo, K., Ito, K., Koh, G. Y., and Suda, T. (2004) Tie2/angiopoietin-1 signaling regulates hematopoietic stem cell quiescence in the bone marrow niche. *Cell* **118**, 149-161
7. Parmar, K., Mauch, P., Vergilio, J. A., Sackstein, R., and Down, J. D. (2007) Distribution of hematopoietic stem cells in the bone marrow according to regional hypoxia. *Proc Natl Acad Sci U S A* **104**, 5431-5436
8. Simsek, T., Kocabas, F., Zheng, J., Deberardinis, R. J., Mahmoud, A. I., Olson, E. N., Schneider, J. W., Zhang, C. C., and Sadek, H. A. (2010) The distinct metabolic profile of hematopoietic stem cells reflects their location in a hypoxic niche. *Cell Stem Cell* **7**, 380-390
9. Takubo, K., Goda, N., Yamada, W., Iriuchishima, H., Ikeda, E., Kubota, Y., Shima, H., Johnson, R. S., Hirao, A., Suematsu, M., and Suda, T. (2010) Regulation of the HIF-1alpha level is essential for hematopoietic stem cells. *Cell Stem Cell* **7**, 391-402
10. Shima, H., Takubo, K., Tago, N., Iwasaki, H., Arai, F., Takahashi, T., and Suda, T. (2010) Acquisition of G(0) state by CD34-positive cord blood cells after bone marrow transplantation. *Exp Hematol* **38**, 1231-1240
11. Trumpp, A., Essers, M., and Wilson, A. (2010) Awakening dormant haematopoietic stem cells. *Nat Rev Immunol* **10**, 201-209
12. Papayannopoulou, T., Priestley, G. V., and Nakamoto, B. (1998) Anti-VLA4/VCAM-1-induced mobilization requires cooperative signaling through the kit/mkit ligand pathway. *Blood* **91**, 2231-2239
13. Heissig, B., Hattori, K., Dias, S., Friedrich, M., Ferris, B., Hackett, N. R., Crystal, R. G., Besmer, P., Lyden, D., Moore, M. A., Werb, Z., and Rafii, S. (2002) Recruitment of stem and progenitor cells from the bone marrow niche requires MMP-9 mediated release of kit-ligand. *Cell* **109**, 625-637
14. Driessen, R. L., Johnston, H. M., and Nilsson, S. K. (2003) Membrane-bound stem cell factor is a key regulator in the initial lodgment of stem cells within the endosteal marrow region. *Exp Hematol* **31**, 1284-1291
15. Bradfute, S. B., Graubert, T. A., and Goodell, M. A. (2005) Roles of Sca-1 in hematopoietic stem/progenitor cell function. *Exp Hematol* **33**, 836-843
16. Suzuki, A., Andrew, D. P., Gonzalo, J. A., Fukumoto, M., Spellberg, J., Hashiyama, M., Takimoto, H., Gerwin, N., Webb, I., Molineux, G., Amakawa, R., Tada, Y., Wakeham, A., Brown, J., McNiece, I., Ley, K., Butcher, E. C., Suda, T., Gutierrez-Ramos, J. C., and Mak, T. W. (1996) CD34-deficient mice have reduced eosinophil accumulation after allergen exposure

and show a novel crossreactive 90-kD protein. *Blood* **87**, 3550-3562

17. Tjwa, M., Sidenius, N., Moura, R., Jansen, S., Theunissen, K., Andolfo, A., De Mol, M., Dewerchin, M., Moons, L., Blasi, F., Verfaillie, C., and Carmeliet, P. (2009) Membrane-anchored uPAR regulates the proliferation, marrow pool size, engraftment, and mobilization of mouse hematopoietic stem/progenitor cells. *J Clin Invest* **119**, 1008-1018
18. Bene, M. C., Castoldi, G., Knapp, W., Rigolin, G. M., Escribano, L., Lemez, P., Ludwig, W. D., Matutes, E., Orfao, A., Lanza, F., and van't Veer, M. (2004) CD87 (urokinase-type plasminogen activator receptor), function and pathology in hematological disorders: a review. *Leukemia* **18**, 394-400
19. Lewis, J. S., Lee, J. A., Underwood, J. C., Harris, A. L., and Lewis, C. E. (1999) Macrophage responses to hypoxia: relevance to disease mechanisms. *J Leukoc Biol* **66**, 889-900
20. Yamazaki, H., Bujo, H., Kusunoki, J., Seimiya, K., Kanaki, T., Morisaki, N., Schneider, W. J., and Saito, Y. (1996) Elements of neural adhesion molecules and a yeast vacuolar protein sorting receptor are present in a novel mammalian low density lipoprotein receptor family member. *J Biol Chem* **271**, 24761-24768
21. Jiang, M., Bujo, H., Ohwaki, K., Unoki, H., Yamazaki, H., Kanaki, T., Shibasaki, M., Azuma, K., Harigaya, K., Schneider, W. J., and Saito, Y. (2008) Ang II-stimulated migration of vascular smooth muscle cells is dependent on LR11 in mice. *J Clin Invest* **118**, 2733-2746
22. Ohwaki, K., Bujo, H., Jiang, M., Yamazaki, H., Schneider, W. J., and Saito, Y. (2007) A secreted soluble form of LR11, specifically expressed in intimal smooth muscle cells, accelerates formation of lipid-laden macrophages. *Arterioscler Thromb Vasc Biol* **27**, 1050-1056
23. Jacobsen, L., Madsen, P., Moestrup, S. K., Lund, A. H., Tommerup, N., Nykjaer, A., Sottrup-Jensen, L., Gliemann, J., and Petersen, C. M. (1996) Molecular characterization of a novel human hybrid-type receptor that binds the alpha2-macroglobulin receptor-associated protein. *J Biol Chem* **271**, 31379-31383
24. Hermey, G., Sjogaard, S. S., Petersen, C. M., Nykjaer, A., and Gliemann, J. (2006) Tumour necrosis factor alpha-converting enzyme mediates ectodomain shedding of Vps10p-domain receptor family members. *Biochem J* **395**, 285-293
25. Bujo, H., and Saito, Y. (2006) Modulation of smooth muscle cell migration by members of the low-density lipoprotein receptor family. *Arterioscler Thromb Vasc Biol* **26**, 1246-1252
26. Zhang, X., Dormady, S. P., and Basch, R. S. (2000) Identification of four human cDNAs that are differentially expressed by early hematopoietic progenitors. *Exp Hematol* **28**, 1286-1296
27. Sakai, S., Nakaseko, C., Takeuchi, M., Ohwada, C., Shimizu, N., Tsukamoto, S., Kawaguchi, T., Jiang, M., Sato, Y., Ebinuma, H., Yokote, K., Iwama, A., Fukamachi, I., Schneider, W. J., Saito, Y., and Bujo, H. (2012) Circulating soluble LR11/SorLA levels are highly increased and ameliorated by chemotherapy in acute leukemias. *Clin Chim Acta* **413**, 1542-1548
28. Matsuo, M., Ebinuma, H., Fukamachi, I., Jiang, M., Bujo, H., and Saito, Y. (2009) Development of an immunoassay for the quantification of soluble LR11, a circulating marker of atherosclerosis. *Clin Chem* **55**, 1801-1808
29. Taira, K., Bujo, H., Hirayama, S., Yamazaki, H., Kanaki, T., Takahashi, K., Ishii, I., Miida, T., Schneider, W. J., and Saito, Y. (2001) LR11, a mosaic LDL receptor family member, mediates the uptake of ApoE-rich lipoproteins in vitro. *Arterioscler Thromb Vasc Biol* **21**, 1501-1506
30. Katayama, K., Wada, K., Miyoshi, H., Ohashi, K., Tachibana, M., Furuki, R., Mizuguchi, H., Hayakawa, T., Nakajima, A., Kadowaki, T., Tsutsumi, Y., Nakagawa, S., Kamisaki, Y., and Mayumi, T. (2004) RNA interfering approach for clarifying the PPARgamma pathway using lentiviral vector expressing short hairpin RNA. *FEBS Lett* **560**, 178-182
31. Zhong, H., and Simons, J. W. (1999) Direct comparison of GAPDH, beta-actin, cyclophilin, and 28S rRNA as internal standards for quantifying RNA levels under hypoxia. *Biochem*

Biophys Res Commun **259**, 523-526

32. Kong, T., Eltzschig, H. K., Karhausen, J., Colgan, S. P., and Shelley, C. S. (2004) Leukocyte adhesion during hypoxia is mediated by HIF-1-dependent induction of beta2 integrin gene expression. *Proc Natl Acad Sci U S A* **101**, 10440-10445
33. Sundstrom, C., and Nilsson, K. (1976) Establishment and characterization of a human histiocytic lymphoma cell line (U-937). *Int J Cancer* **17**, 565-577
34. Arai, F., and Suda, T. (2007) Maintenance of quiescent hematopoietic stem cells in the osteoblastic niche. *Ann N Y Acad Sci* **1106**, 41-53
35. Jang, Y. Y., and Sharkis, S. J. (2007) A low level of reactive oxygen species selects for primitive hematopoietic stem cells that may reside in the low-oxygenic niche. *Blood* **110**, 3056-3063
36. Krishnamachary, B., Berg-Dixon, S., Kelly, B., Agani, F., Feldser, D., Ferreira, G., Iyer, N., LaRusch, J., Pak, B., Taghavi, P., and Semenza, G. L. (2003) Regulation of colon carcinoma cell invasion by hypoxia-inducible factor 1. *Cancer Res* **63**, 1138-1143
37. Lester, R. D., Jo, M., Montel, V., Takimoto, S., and Gonias, S. L. (2007) uPAR induces epithelial-mesenchymal transition in hypoxic breast cancer cells. *J Cell Biol* **178**, 425-436
38. Smith, H. W., and Marshall, C. J. (2010) Regulation of cell signalling by uPAR. *Nat Rev Mol Cell Biol* **11**, 23-36
39. Wang, G. L., Jiang, B. H., Rue, E. A., and Semenza, G. L. (1995) Hypoxia-inducible factor 1 is a basic-helix-loop-helix-PAS heterodimer regulated by cellular O2 tension. *Proc Natl Acad Sci U S A* **92**, 5510-5514
40. Benita, Y., Kikuchi, H., Smith, A. D., Zhang, M. Q., Chung, D. C., and Xavier, R. J. (2009) An integrative genomics approach identifies Hypoxia Inducible Factor-1 (HIF-1)-target genes that form the core response to hypoxia. *Nucleic Acids Res* **37**, 4587-4602
41. Zhu, Y., Bujo, H., Yamazaki, H., Hirayama, S., Kanaki, T., Takahashi, K., Shibasaki, M., Schneider, W. J., and Saito, Y. (2002) Enhanced expression of the LDL receptor family member LR11 increases migration of smooth muscle cells in vitro. *Circulation* **105**, 1830-1836
42. Zhu, Y., Bujo, H., Yamazaki, H., Ohwaki, K., Jiang, M., Hirayama, S., Kanaki, T., Shibasaki, M., Takahashi, K., Schneider, W. J., and Saito, Y. (2004) LR11, an LDL receptor gene family member, is a novel regulator of smooth muscle cell migration. *Circ Res* **94**, 752-758
43. Willnow, T. E., Petersen, C. M., and Nykjaer, A. (2008) VPS10P-domain receptors - regulators of neuronal viability and function. *Nat Rev Neurosci* **9**, 899-909
44. Rogaeva, E., Meng, Y., Lee, J. H., Gu, Y., Kawarai, T., Zou, F., Katayama, T., Baldwin, C. T., Cheng, R., Hasegawa, H., Chen, F., Shibata, N., Lunetta, K. L., Pardossi-Piquard, R., Bohm, C., Wakutani, Y., Cupples, L. A., Cuenco, K. T., Green, R. C., Pinessi, L., Rainero, I., Sorbi, S., Bruni, A., Duara, R., Friedland, R. P., Inzelberg, R., Hampe, W., Bujo, H., Song, Y. Q., Andersen, O. M., Willnow, T. E., Graff-Radford, N., Petersen, R. C., Dickson, D., Der, S. D., Fraser, P. E., Schmitt-Ulms, G., Younkin, S., Mayeux, R., Farrer, L. A., and St George-Hyslop, P. (2007) The neuronal sortilin-related receptor SORL1 is genetically associated with Alzheimer disease. *Nat Genet* **39**, 168-177
45. Ikeuchi, T., Hirayama, S., Miida, T., Fukamachi, I., Tokutake, T., Ebinuma, H., Takubo, K., Kaneko, H., Kasuga, K., Kakita, A., Takahashi, H., Bujo, H., Saito, Y., and Nishizawa, M. (2010) Increased levels of soluble LR11 in cerebrospinal fluid of patients with Alzheimer disease. *Dement Geriatr Cogn Disord* **30**, 28-32
46. Harrison, J. S., Rameshwar, P., Chang, V., and Bandari, P. (2002) Oxygen saturation in the bone marrow of healthy volunteers. *Blood* **99**, 394
47. Cipolleschi, M. G., Dello Sbarba, P., and Olivotto, M. (1993) The role of hypoxia in the maintenance of hematopoietic stem cells. *Blood* **82**, 2031-2037

48. Danet, G. H., Pan, Y., Luongo, J. L., Bonnet, D. A., and Simon, M. C. (2003) Expansion of human SCID-repopulating cells under hypoxic conditions. *J Clin Invest* **112**, 126-135
49. Ivanovic, Z., Hermitte, F., Brunet de la Grange, P., Dazey, B., Belloc, F., Lacombe, F., Vezon, G., and Praloran, V. (2004) Simultaneous maintenance of human cord blood SCID-repopulating cells and expansion of committed progenitors at low O2 concentration (3%). *Stem Cells* **22**, 716-724
50. Hermitte, F., Brunet de la Grange, P., Belloc, F., Praloran, V., and Ivanovic, Z. (2006) Very low O2 concentration (0.1%) favors G0 return of dividing CD34+ cells. *Stem Cells* **24**, 65-73
51. Goodell, M. A., Brose, K., Paradis, G., Conner, A. S., and Mulligan, R. C. (1996) Isolation and functional properties of murine hematopoietic stem cells that are replicating in vivo. *J Exp Med* **183**, 1797-1806
52. Krishnamurthy, P., Ross, D. D., Nakanishi, T., Bailey-Dell, K., Zhou, S., Mercer, K. E., Sarkadi, B., Sorrentino, B. P., and Schuetz, J. D. (2004) The stem cell marker Bcrp/ABCG2 enhances hypoxic cell survival through interactions with heme. *J Biol Chem* **279**, 24218-24225
53. Kirito, K., Fox, N., Komatsu, N., and Kaushansky, K. (2005) Thrombopoietin enhances expression of vascular endothelial growth factor (VEGF) in primitive hematopoietic cells through induction of HIF-1alpha. *Blood* **105**, 4258-4263
54. Pedersen, M., Lofstedt, T., Sun, J., Holmquist-Mengelbier, L., Pahlman, S., and Ronnstrand, L. (2008) Stem cell factor induces HIF-1alpha at normoxia in hematopoietic cells. *Biochem Biophys Res Commun* **377**, 98-103
55. Winning, S., Splettstoesser, F., Fandrey, J., and Frede, S. (2010) Acute hypoxia induces HIF-independent monocyte adhesion to endothelial cells through increased intercellular adhesion molecule-1 expression: the role of hypoxic inhibition of prolyl hydroxylase activity for the induction of NF-kappa B. *J Immunol* **185**, 1786-1793

Acknowledgments—We thank Dr. M. Watanabe (Tokyo New Drug Research Laboratories, Pharmaceutical Division, Kowa Co. Ltd.) for his excellent technical assistance.

FOOTNOTES

*This study was supported by Health and Labor Sciences Research Grants for Translational Research, Japan (H. B.) and the grants from Japanese Ministry of Education, Culture, Sports, Science and Technology (H. B.). W.J.S. was supported by grants of the Austrian Science Fund (FWF).
[1]To whom correspondence should be addressed: Hideaki Bujo, MD, Department of Genome Research and Clinical Application, Chiba University Graduate School of Medicine, 1-8-1 Inohana, Chiba 260-8670, Japan, Phone: 81-43-222-7171; Fax: 81-43-226-2095; E-mail: hbujo@faculty.chiba-u.jp
[2]Department of Hematology, Chiba University Hospital, Chiba, Japan.
[3]Division of Transfusion Medicine and Cell Therapy, Chiba University Hospital, Chiba, Japan.
[4]Department of Medical Biochemistry, Max F. Perutz Laboratories, Medical University of Vienna, Vienna, Austria.

FIGURE LEGENDS

FIGURE 1. Hypoxia induces expression of LR11 in HSPCs. After incubation for 24 h or 48 h under normoxic or hypoxic conditions, the LR11 expression levels in c-Kit(+) Lin(-) cells and Lin(+) cells were evaluated by immunoblot analysis as described in "Experimental Procedures". The LR11-specific signals at 250 kDa were quantified using the Image-Lab software. The blot shown is representative of 3 independent experiments. Data are presented as mean ± SD (n=3). * $p<0.05$; ns, not significant.

FIGURE 2. Effects of hypoxia on LR11 mRNA levels and on sLR11 production by U937 cells. A. LR11 mRNA expression in U937 cells after incubation under normoxic or hypoxic conditions for 3, 6, and 24 h were analyzed by quantitative PCR as described in "Experimental Procedures". mRNA levels are represented as fold increase of those at 0 h. Data are presented as mean ± SD (n=3). * $p<0.05$; ns, not significant. B. After incubation under normoxic or hypoxic conditions for 6, 24, and 48 h, LR11 expression levels in U937 cells were analyzed by immunoblot analysis. The LR11-specific signals at 250 kDa were quantified using the Image-Lab software. The blot shown is representative of 3 independent experiments. Data are presented as mean ± SD (n=3). * $p<0.05$; ns, not significant. C. The concentrations of sLR11 in conditioned media of U937 cells incubated under normoxic or hypoxic condition for 48 h were determined by ELISA as described in "Experimental Procedures". Data are presented as mean ± SD (n=3). * $p<0.05$.

FIGURE 3. Effects of manipulating LR11 levels on the hypoxia-induced adhesion of immature hematological cells. A. After incubation in hypoxic or normoxic conditions for 24 h, the numbers of attached U937 cells, either transfected with shRNA specific for LR11 (#1 or #5) or with control shRNA (Ctrl), to MSCs were determined as described in "Experimental Procedures". Inset: LR11 levels in normal and LR11-knockdown U937 cells were analyzed by immunoblot. Data are shown as -fold increase of those at control cells without hypoxic conditions and presented as mean ± SD (n=3). * $p<0.05$; ns, not significant. B. After incubation in normoxic or hypoxic conditions for 24 h, the numbers of c-Kit(+) Lin(-) cells prepared from *LR11*$^{+/+}$ or *LR11*$^{-/-}$ mice attached to OP-9 cells were determined as described in "Experimental Procedures". Data are presented as mean ± SD (n=3). * $p<0.05$.

FIGURE 4. Effects of sLR11 on HSPC adhesion to bone marrow stromal cells. A. U937 cells pre-incubated for 2 h with the indicated concentrations of sLR11 were subjected to analyses of their adhesion to plates coated with MSCs as described in "Experimental Procedures". B. Cells transiently transfected with cDNA specific for LR11 or with an empty vector (mock) were subjected to adhesion analyses as described for panel *A*. Inset: LR11 expression of mock-transfected and LR11-overexpressing U937 cells were analyzed by immunoblotting. C. c-Kit(+) Lin(-) cells pre-incubated for 15 min with the indicated concentrations of sLR11 were subjected to analyses of their adhesion to plates coated with OP-9 cells as described in "Experimental Procedures". In panels A to C, the numbers of attached cells are presented as -fold increase of those under control conditions (Mean ± SD, n=3). * $p<0.05$; ns, not significant.

FIGURE 5. Significance of LR11/uPAR-complex formation in hypoxia-induced adhesion of U937 cells. A. U937 cells (left panel) or c-Kit(+) Lin(-) cells (right panel) pre-incubated for 2 h with the indicated concentrations of sLR11 were subjected to analyses of their adhesion to plates coated with vitronectin as described in "Experimental Procedures". The numbers of attached cells are presented as -fold increase over those without sLR11 (Mean ± SD, n=3). * $p<0.05$; ns, not significant. B. U937 cells pre-incubated for 4 h with or without 1 ng/ml sLR11 in the presence of anti-uPAR neutralizing antibody (αuPAR) or of control IgG (C. IgG) were subjected to analyses of their adhesion to plates coated with MSCs as described in "Experimental Procedures". The numbers of attached cells are presented as -fold increase of those without sLR11 or without antibodies (Mean ± SD, n=3). * $p<0.05$; ns, not significant. C. U937 cells pre-incubated for 24 h under normoxic or hypoxic conditions were incubated with 10 ng/ml sLR11 for 15min, the cell lysates were immunoprecipitated with the monoclonal anti-LR11 antibody M3 (αLR11) or with control IgG (C. IgG) and subjected to immunoblot analysis with the monoclonal anti-LR11 antibody A2-2-3 or with polyclonal antibodies against uPAR, respectively, as described in "Experimental Procedures". The signals for LR11 (250 kDa) or uPAR (65 kDa) were quantified using the Image-Lab software. D. K562 cells stably transfected with cDNA specific for LR11 or vector alone (mock) were subjected to flow cytometric analysis as described in "Experimental Procedures". The profiles of surface uPAR expression are presented in histograms. The frequencies and the mean fluorescence intensities (MFIs) of the fractions of cells with high uPAR levels are indicated. The filled histograms are isotype controls. Representative data from multiple experiments are shown. Inset: LR11 levels in control or LR11-overexpressing K562 cells were analyzed by immunoblot using the monoclonal anti-LR11 antibody, A2-2-3.

FIGURE 6. Functional link between HIF-1α and LR11 in enhancing hypoxia-induced cell adhesion. A. After incubation for 24 h under normoxic or hypoxic conditions (1% O_2 and 5% CO_2), LR11 and HIF-1α protein levels were evaluated by immunoblot analysis with the monoclonal anti-LR11 antibody A2-2-3, or with polyclonal antibodies against HIF-1α, respectively, as described in "Experimental Procedures". The specific signals for LR11 (250 kDa) and HIF-1α (120 kDa) were quantified using the Image-Lab software. B. U937 cells incubated for 48 h with the indicated concentrations of $CoCl_2$ were subjected to immunoblot analysis using monoclonal anti-LR11 antibody A2-2-3 as described in "Experimental Procedures". The LR11-specific signals at 250 kDa were quantified using the Image-Lab software. The blot shown is representative of 3 independent experiments. Data are presented as mean ± SD (n=3). * $p<0.05$; ns, not significant. C. Conditioned media collected after incubation for 48 h with the indicated concentrations of $CoCl_2$ were concentrated and subjected to sLR11 measurement by ELISA as described in "Experimental Procedures". Data are presented as mean ± SD (n=3). * $p<0.05$; ns, not significant. D. After incubation in normoxic or hypoxic conditions for 24 h with or without 1 ng/ml sLR11, the numbers of U937 cells previously transfected with siRNA specific for HIF-1α or with control siRNA attached to

MSCs were counted. U937 cells incubated for 4 h in the presence or absence of 1 ng/ml sLR11 after pre-incubation for 24 h under normoxic or hypoxic conditions were subjected to analyses of their adhesion to plates coated with MSCs as described in "Experimental Procedures". Data are shown as -fold increase compared to control cells in the absence of sLR11 under normoxia. Data are presented as mean ± SD (n=3). * $p<0.05$; ns, not significant.

FIGURE 7. Binding of HIF-1α to the potential binding site in the CD18 promoter. A. The nucleotide sequence including a potential HIF-1α binding site within the LR11 gene promoter is shown. The motif 5′ -ACGTG-3′ spanning nucleotides -65 to -61 is boxed, and the sequences corresponding to the forward and reverse primers are shown with arrows. B. HIF-1α binding to the LR11 and CD18 promoter in normoxic and hypoxic conditions was examined using chromatin immunoprecipitation (ChIP) analysis in U937 cells. Chromatin-associated DNA (Input) prior to immunoprecipitation with anti- HIF-1α antibody was used for PCR controls. The amplified products were consistent with the expected size of fragments for LR11 (144 bp) and CD18 (166 bp) promoters, and the amplified sequences were confirmed to be identical to those expected, respectively. The photo shown is representative of 3 independent experiments.

Figure 1

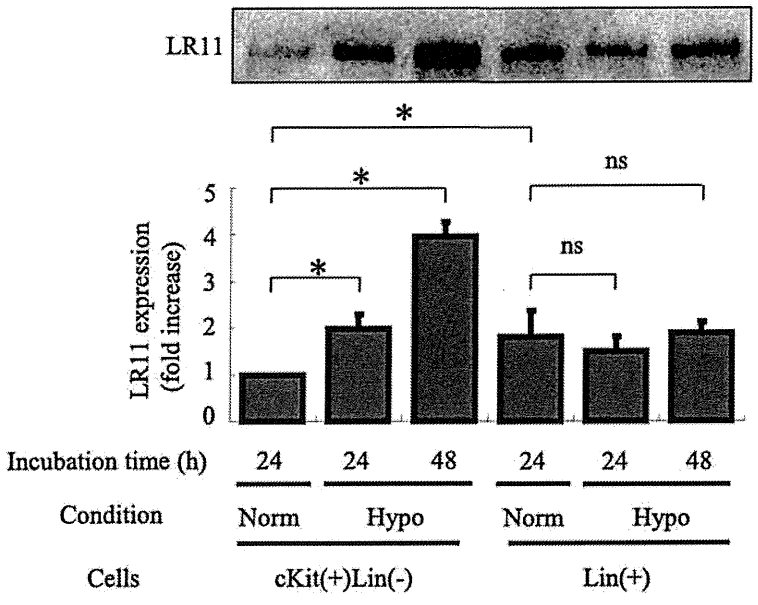
LR11
*
*
*
ns
ns
LR11 expression (fold increase)
0
1
2
3
4
5
Incubation time (h)
24
24
48
24
24
48
Condition
Norm
Hypo
Norm
Hypo
Cells
cKit(+)Lin(-)
Lin(+)

Figure 2

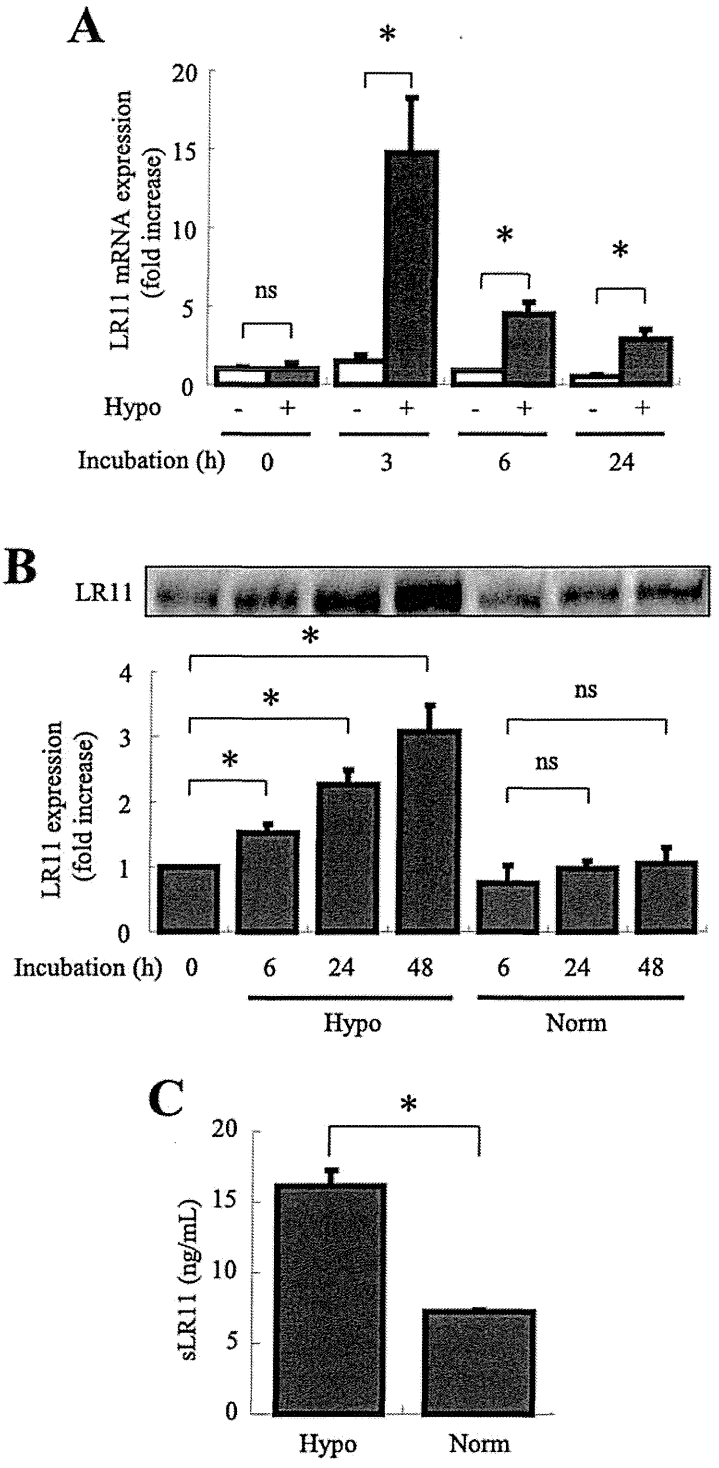
A
LR11 mRNA expression (fold increase)
20
15
10
5
0
ns
*
*
*
Hypo
- + - + - + - +
Incubation (h) 0 3 6 24
B
LR11
LR11 expression (fold increase)
4
3
2
1
0
*
*
*
ns
ns
Incubation (h) 0 6 24 48 6 24 48
Hypo
Norm
C
sLR11 (ng/mL)
20
15
10
5
0
*
Hypo
Norm

Figure 3

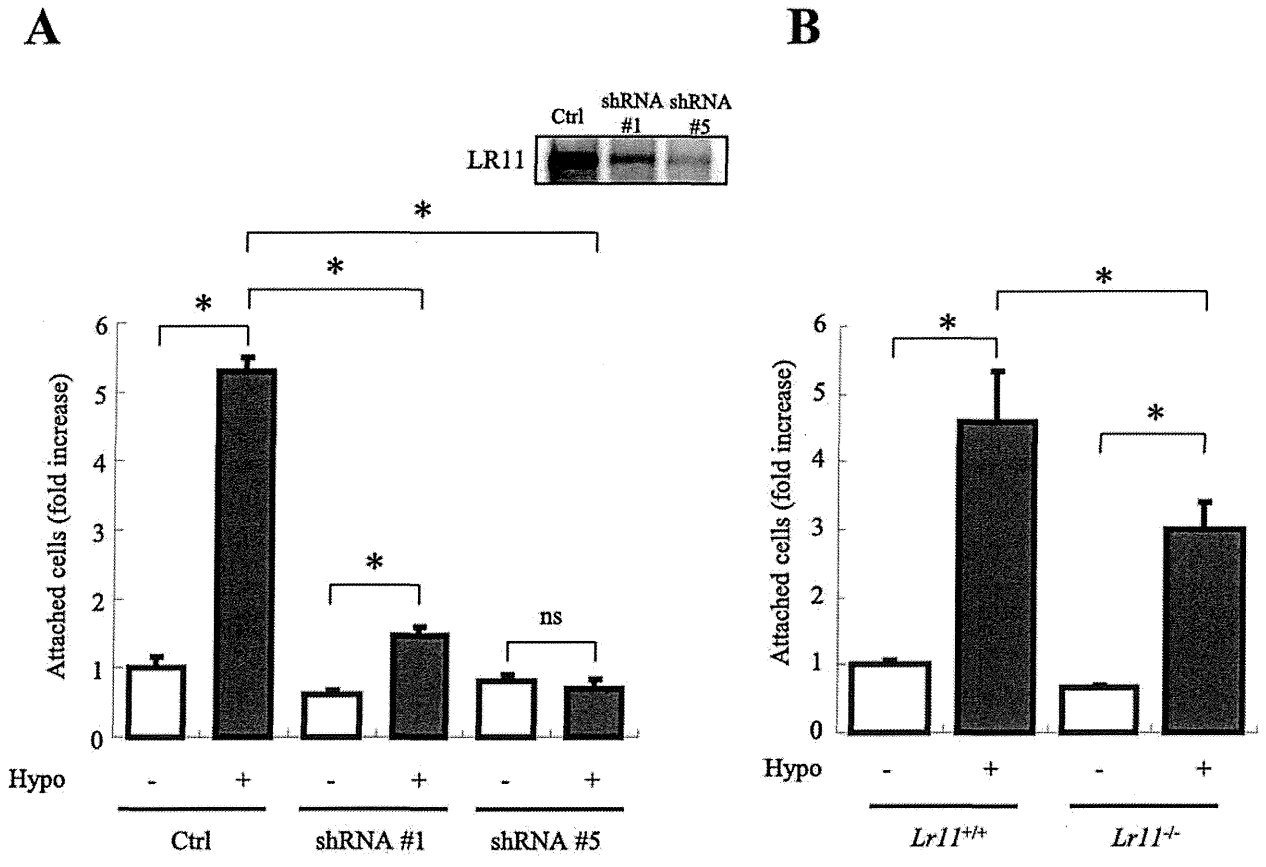
A
B
Ctrl
shRNA #1
shRNA #5
LR11
Attached cells (fold increase)
Hypo
ns
Ctrl
shRNA #1
shRNA #5
Lr11+/+
Lr11-/-

Figure 4

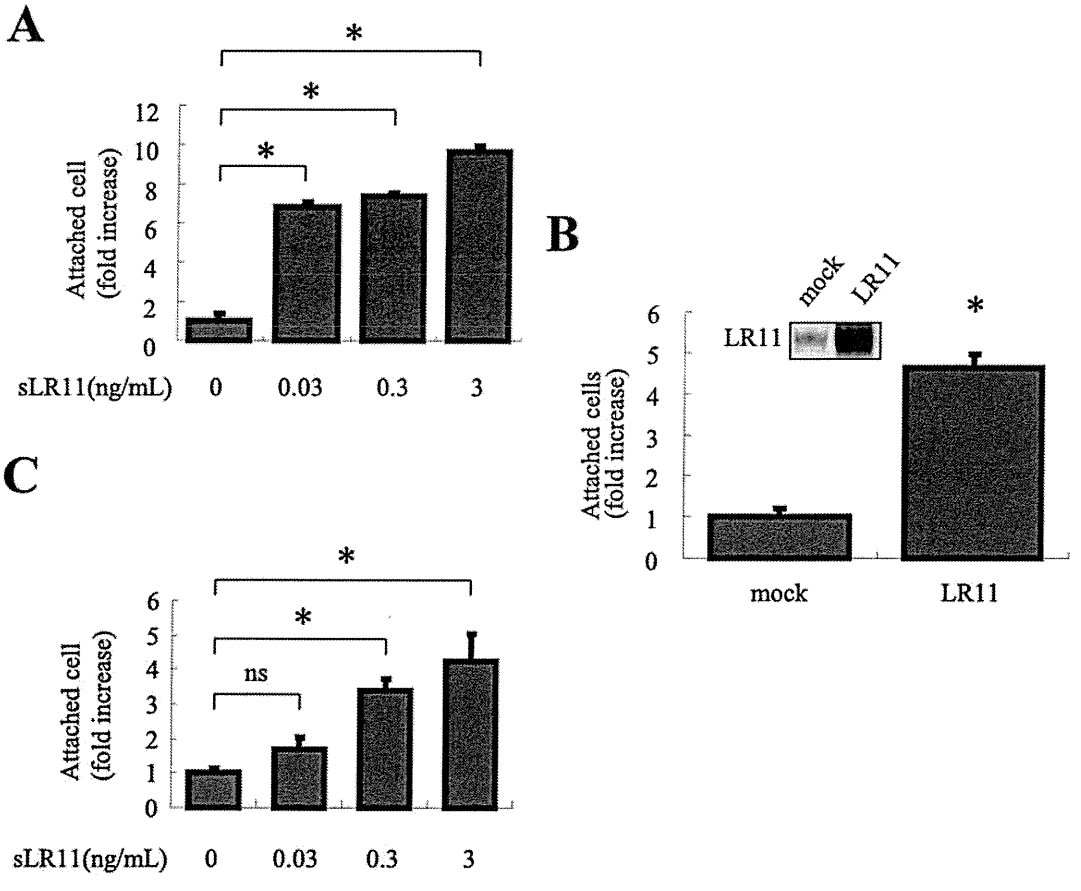
A
*
*
*
12
10
8
6
4
2
0
Attached cell (fold increase)
sLR11(ng/mL) 0 0.03 0.3 3
B
mock
LR11
LR11
*
6
5
4
3
2
1
0
Attached cells (fold increase)
mock
LR11
C
*
*
ns
6
5
4
3
2
1
0
Attached cell (fold increase)
sLR11(ng/mL) 0 0.03 0.3 3

Figure 5

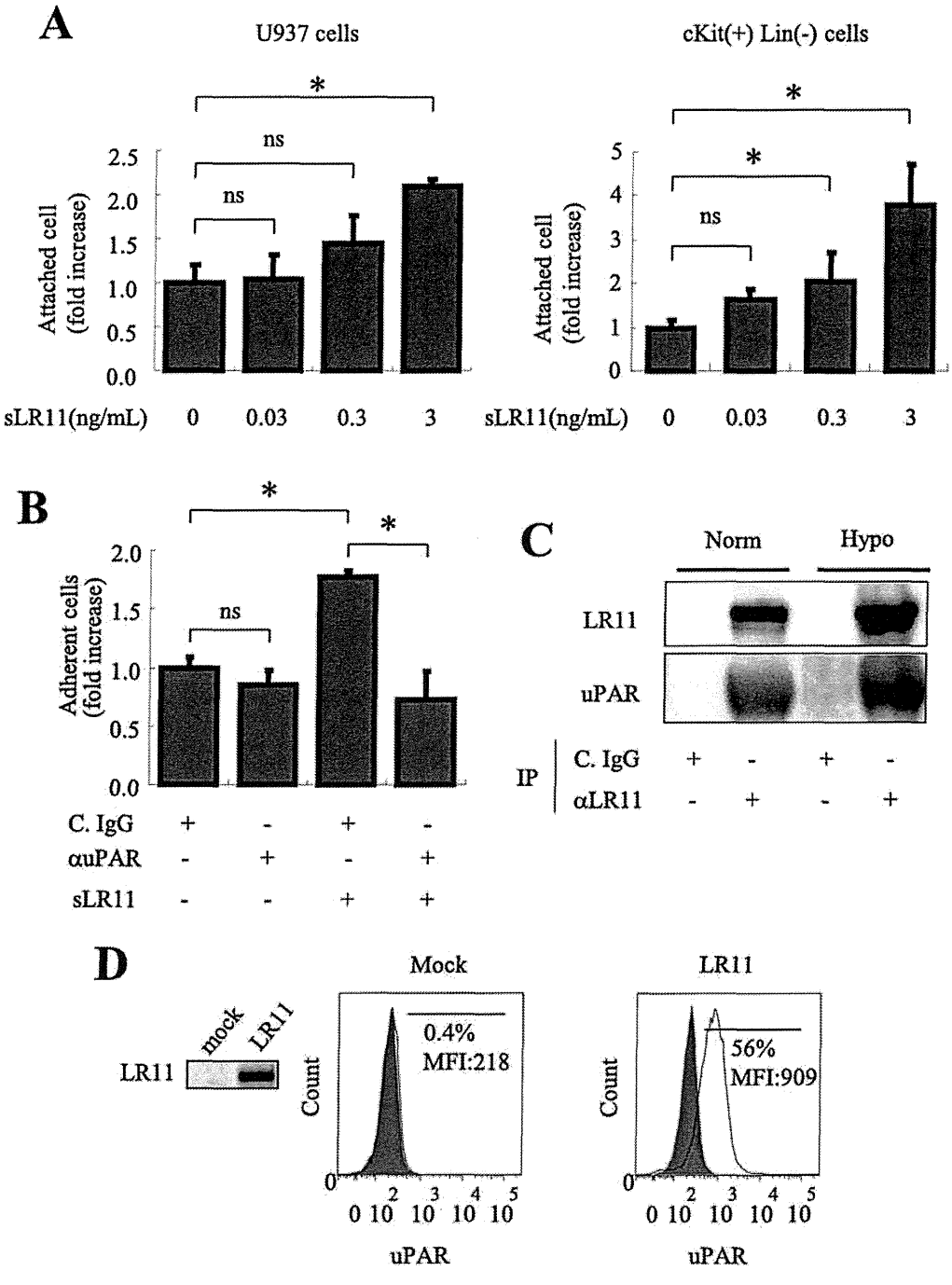
A
U937 cells
cKit(+) Lin(-) cells
Attached cell (fold increase)
ns
*
sLR11(ng/mL) 0 0.03 0.3 3
B
Adherent cells (fold increase)
C. IgG
αuPAR
sLR11
C
Norm
Hypo
LR11
uPAR
IP
C. IgG
αLR11
D
mock
LR11
Mock
0.4%
MFI:218
56%
MFI:909
Count
uPAR

Figure 6

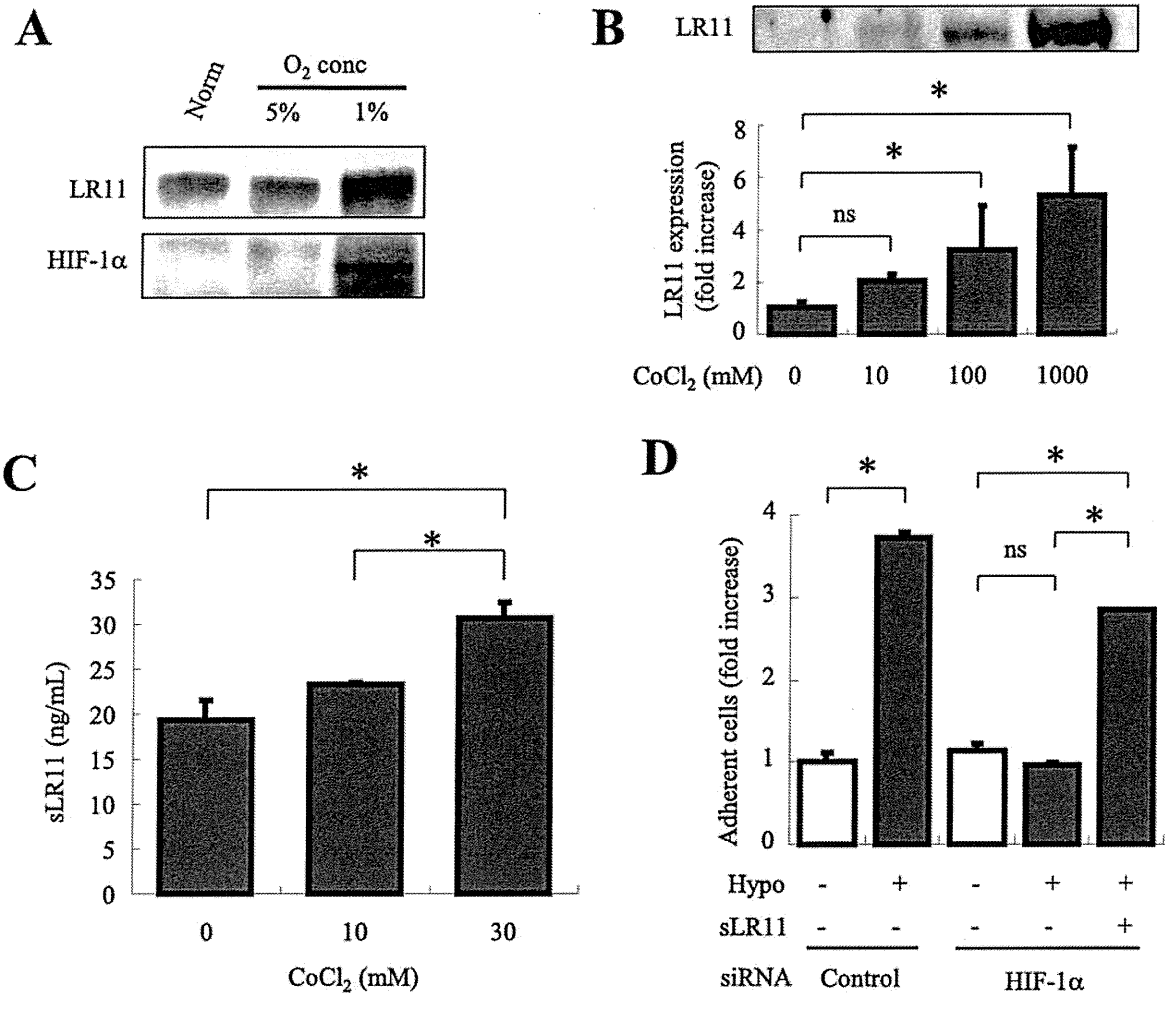
A
Norm
O_2 conc
5%
1%
LR11
HIF-1α
B
LR11
LR11 expression (fold increase)
ns
$CoCl_2$ (mM) 0 10 100 1000
C
sLR11 (ng/mL)
$CoCl_2$ (mM)
0
10
30
D
Adherent cells (fold increase)
Hypo
sLR11
siRNA
Control
HIF-1α
ns

Figure 7

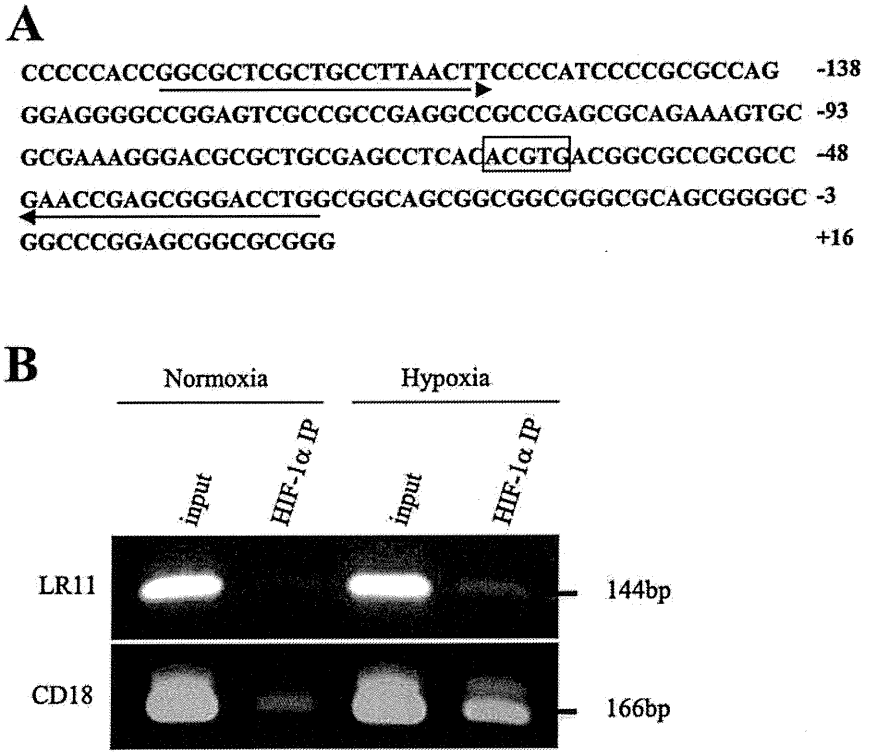
A
CCCCCACCGGCGCTCGCTGCCTTAACTTCCCCATCCCCGCGCCAG -138
GGAGGGGCCGGAGTCGCCGCCGAGGCCGCCGAGCGCAGAAAGTGC -93
GCGAAAGGGACGCGCTGCGAGCCTCACACGTGACGGCGCCGCGCC -48
GAACCGAGCGGGACCTGGCGGCAGCGGCGGCGGGCGCAGCGGGGC -3
GGCCCGGAGCGGCGCGGG +16
B
Normoxia
Hypoxia
input
HIF-1α IP
input
HIF-1α IP
LR11
144bp
CD18
166bp

Acta Crystallographica Section F
Structural Biology and Crystallization Communications
ISSN 1744-3091

Crystallization and preliminary crystallographic analysis of human LR11 Vps10p domain

Zenzaburo Nakata,[a] Masamichi Nagae,[a] Norihisa Yasui,[a]‡ Hideaki Bujo,[b] Terukazu Nogi[a] and Junichi Takagi[a]*

[a]Laboratory of Protein Synthesis and Expression, Institute for Protein Research, Osaka University, 3-2 Yamadaoka, Suita, Osaka 565-0871, Japan, and [b]Department of Genome Research and Clinical Application (M6), Graduate School of Medicine, Chiba University, 1-8-1 Inohana, Chuo-ku, Chiba 260-8670, Japan

‡ Present address: Department of Biochemistry and Molecular Biology, The University of Chicago, 929 East 57th Street, Chicago, IL 60637, USA.

Correspondence e-mail: takagi@protein.osaka-u.ac.jp

Received 4 October 2010
Accepted 18 November 2010

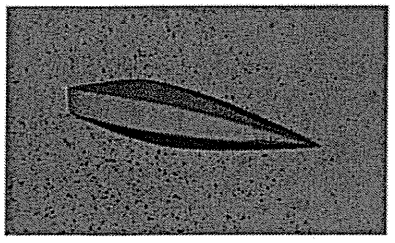

Low-density lipoprotein receptor (LDLR) relative with 11 binding repeats (LR11; also known as sorLA) is genetically associated with late-onset Alzheimer's disease and is thought to be involved in neurodegenerative processes. LR11 contains a vacuolar protein-sorting 10 protein (Vps10p) domain. As this domain has been implicated in protein–protein interaction in other receptors, its structure and function are of great biological interest. Human LR11 Vps10p domain was expressed in mammalian cells and the purified protein was crystallized using the hanging-drop vapour-diffusion method. Enzymatic deglycosylation of the sample was critical to obtaining diffraction-quality crystals. Deglycosylated LR11 Vps10p-domain crystals belonged to the hexagonal space group $P6_122$. A diffraction data set was collected to 2.4 Å resolution and a clear molecular-replacement solution was obtained.

1. Introduction

LDLR relative with 11 binding repeats (LR11) is a type 1 membrane protein that is expressed abundantly in the central as well as the peripheral nervous system and to a lesser extent in other organs (Hermans-Borgmeyer *et al.*, 1998; Yamazaki *et al.*, 1996; Motoi *et al.*, 1999). LR11 expression is selectively reduced in the brains of Alzheimer's disease (AD) patients (Scherzer *et al.*, 2004). Genetic studies have also revealed a strong association of LR11 genetic variants with the risk of AD in several populations (Rogaeva *et al.*, 2007; Lee *et al.*, 2007; Bettens *et al.*, 2008). Although the exact molecular mechanism underlying these phenomena is still unclear, LR11 has been hypothesized to be involved in the intracellular trafficking of amyloid precursor protein (APP) between the trans-Golgi network and early endosomes (Andersen *et al.*, 2005; Willnow *et al.*, 2008), reducing the chance of APP processing in the late endosomes. In fact, overexpression of LR11 in HEK293 cells reduced the levels of extracellular amyloid β peptide produced (Offe *et al.*, 2006). In addition to direct interaction with APP during this trafficking (Andersen *et al.*, 2006), LR11 may also directly interact with β-secretase, blocking the β-secretase–APP interaction (Spoelgen *et al.*, 2006).

Uniquely among the LDLR gene family proteins, LR11 possesses an ~700-amino-acid domain that was initially identified in the vacuolar protein-sorting 10 protein (Vps10p), a sorting protein in yeast that transports carboxypeptidase Y from the Golgi to the vacuole (Marcusson *et al.*, 1994). Mammalian receptors that contain this domain constitute another family of proteins that are highly expressed in neuronal tissues (Willnow *et al.*, 2008). Sortilin is the most extensively studied member of this family and is thought to be involved in the intracellular sorting of brain-derived neurotrophic factor (Chen *et al.*, 2005). The crystal structure of the sortilin Vps10p domain in complex with the neuronal peptide neurotensin has recently been reported (Quistgaard *et al.*, 2009), revealing that the Vps10p domain is comprised of a unique ten-bladed β-propeller fold followed by two small cysteine-rich domains (10CC-a and 10CC-b domains) that make intimate contacts with the bottom face of the propeller. It was also revealed that the ligand peptide is deeply buried in the tunnel of the ten-bladed β-propeller fold. There is no precedent for β-propeller domains with a blade number greater than eight

Table 1
Data-collection and processing statistics.

Values in parentheses are for the highest resolution shell.

No. of crystals	1
Beamline	Photon Factory BL-17A
Wavelength (Å)	0.980
Detector	ADSC Quantum 270
Crystal-to-detector distance (mm)	279.6
Rotation range per image (°)	0.5
Total rotation range (°)	130
Exposure time per image (s)	5
Resolution range (Å)	50–2.4 (2.44–2.40)
Space group	$P6_122$
Unit-cell parameters (Å)	$a = b = 126.4$, $c = 290.3$
Mosaicity (°)	0.251
Total No. of measured intensities	678636
Unique reflections	54346 (2670)
Multiplicity	12.5 (10.2)
Mean $I/\sigma(I)$	15.9
Completeness (%)	99.6 (100.0)
R_{merge}† (%)	5.5 (46.9)
R_{meas} or $R_{r.i.m.}$ (%)	5.8 (43.8)
Overall B factor from Wilson plot (Å^2)	58.3

† $R_{merge} = \sum_{hkl}\sum_i |I_i(hkl) - \langle I(hkl)\rangle| / \sum_{hkl}\sum_i I_i(hkl)$, where $I_i(hkl)$ is the ith intensity of reflection hkl and $\langle I(hkl)\rangle$ is the weighted average intensity for all observations i of reflection hkl.

and the Vps10p domain is probably the largest of the known extracellular modules that fold as a single structural unit (Bork *et al.*, 1996). Given the potential role of the Vps10p domain in the intracellular trafficking exerted by LR11, it is of great biological as well as medical importance to gain insight into the three-dimensional structure of the LR11 Vps10p domain. To this end, here we report the expression, purification, crystallization and preliminary crystallographic analysis of LR11 Vps10p domain.

2. Methods

2.1. Expression and purification of LR11 Vps10p domain

Human LR11 cDNA (gene accession No. NM_003105) was used to amplify the Vps10p domain, corresponding to the N-terminal 753-residue portion (Ohwaki *et al.*, 2007). The primer sequences were 5′-CCG**GAATTC**GCCACCATGGCGACACGGAGCAG-3′ (the *Eco*RI site is shown in bold) and 5′-CG**ATCTAGA**GGGACAGGGGACCAGCTCTCCTTCC-3′ (the *Xba*I site is shown in bold). The resultant PCR product was cloned into the *Eco*RI/*Xba*I site of pcDNA3.1/Myc-His (Invitrogen) that had been modified to include tag sequences at the C-terminus, SRL*ENLYFQ^GG***HHHHHHHHHHIEQKLISEEDLNMHTG**HHHHHHH**, containing a tobacco etch virus (TEV) protease recognition sequence (shown in italics with the cleavage site indicated by a caret) and tandem His-tag (bold) and Myc-tag (underlined) sequences. Using this plasmid, CHO lec 3.2.8.1 cells (Stanley, 1989) were transfected as described previously (Nogi *et al.*, 2006). The transfected cells were plated in 96-well plates and selected for resistance against 1.5 mg ml^{-1} G418. Confluent culture supernatants from the single-colony wells were subjected to immunoblotting using anti-Myc antibody (Invitrogen) and the clone with the highest secretion level of LR11 Vps10p domain was chosen for production-scale culture in roller bottles. The recombinant protein was initially fractionated from the culture medium by ammonium sulfate precipitation (50% saturation), dissolved in wash buffer (20 m*M* Tris pH 8.0, 0.3 *M* NaCl, 50 m*M* imidazole) and applied onto an Ni–NTA agarose column (Qiagen). The column was washed with wash buffer and eluted with elution buffer (20 m*M* Tris pH 8.0, 0.3 *M* NaCl, 0.25 *M* imidazole). The eluted material was dialyzed in buffer *A* (20 m*M* Tris pH 8.0, 50 m*M* NaCl) and incubated with hexahistidine-tagged TEV protease at an enzyme:substrate ratio of 1:15(*w*:*w*) for 16 h at 277 K to remove the C-terminal tag. For deglycosylation, endoglycosidase H (Endo H; New England Biolabs) was added at a ratio of 5 U enzyme per 1 µg substrate protein and was incubated together with TEV protease under the same conditions as described above. The samples were then reapplied onto the Ni–NTA agarose column to remove the cleaved tags and the protease. The flowthrough fractions were collected and applied onto a Mono Q 5/50 GL column (GE Healthcare). The column was equilibrated with buffer *A* and eluted with a linear gradient of NaCl (50–300 m*M*). LR11 Vps10p domain eluted as a single peak at around 150 m*M* NaCl. The purified protein was concentrated to 6 mg ml^{-1} using an Ultrafree-0.5 centrifugal filter (30 kDa molecular-weight cutoff; Millipore). Typical yields ranged between 0.5 and 1.3 mg per litre of culture supernatant.

2.2. Crystallization

Initial screening for crystallization conditions was carried out using Index, Crystal Screen, Crystal Screen 2 and SaltRx from Hampton Research and Wizard Screens I and II from Emerald BioSystems. In these screens, a Mosquito crystallization robot (TTP Labtech) was used to dispense a mixture of 0.1 µl protein solution (LR11 Vps10p domain in 20 m*M* Tris pH 8.0, 150 m*M* NaCl) and 0.1 µl reservoir solution. Drops were equilibrated against 100 µl reservoir solution using the sitting-drop vapour-diffusion method at 293 K. The initial crystallization condition (solution No. 11 of Crystal Screen; 0.1 *M* sodium citrate tribasic pH 5.6, 1.0 *M* ammonium phosphate monobasic) was further optimized using a 24-well crystallization plate with the hanging-drop vapour-diffusion method. Each well contained 350 µl reservoir solution and the drop consisted of a mixture of 0.5 µl protein solution and 0.5 µl reservoir solution.

2.3. Data collection and phasing

For X-ray diffraction experiments, crystals were soaked in reservoir solution containing 20% glycerol or ethylene glycol and flash-cooled in liquid nitrogen. X-ray diffraction data for the crystal grown from the fully glycosylated sample were collected at 100 K on beamline BL44XU at SPring-8 (Harima, Japan) using a wavelength of 0.900 Å and a DIP-6040 imaging-plate detector (Bruker). An X-ray diffraction data set for the crystal grown from the Endo H-treated protein was collected at 95 K on beamline BL-17A at the Photon Factory (Tsukuba, Japan) using a wavelength of 0.980 Å and an ADSC Quantum 270 CCD detector. For the latter, data collection

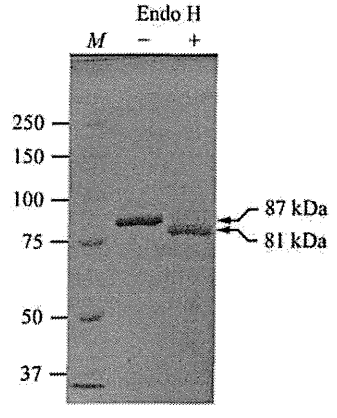

Figure 1
SDS–PAGE analysis of the purified LR11 Vps10p domain before and after Endo H treatment. 2 µg of the purified protein was either treated with 10 U Endo H (+) or left untreated (−) and subjected to SDS–PAGE using 8% gel under reducing conditions followed by staining with Coomassie Brilliant Blue. Lane *M* contains molecular-weight markers (labelled in kDa).

was performed with a total oscillation range of 130° and each diffraction image was obtained with an oscillation angle of 0.5° and an exposure time of 5 s. The diffraction data were processed and scaled using the *HKL*-2000 program suite (Otwinowski & Minor, 1997). Data-collection statistics are listed in Table 1. Phase determination was performed by the molecular-replacement method using the program *MOLREP* (Vagin & Teplyakov, 2010). The initial model was refined with *REFMAC*5 (Murshudov *et al.*, 1997) and a weighted $2F_{obs} - F_{calc}$ electron-density map was calculated using the coefficients produced by *REFMAC*5. Inspection of the crystal packing and the electron-density map was performed with *Coot* (Emsley & Cowtan, 2004).

3. Results and discussion

LR11 Vps10p domain contains six potential N-linked glycosylation sites and seven disulfide bonds, demanding production in a mammalian-cell expression system. We used CHO lec 3.2.8.1 cells as the production host because they are known to produce glycoproteins with homogeneous glycoforms, which is ideal for crystallization (Davis *et al.*, 1993). The relative molecular mass of the purified protein was estimated to be 87 kDa on an SDS–PAGE gel (Fig. 1). The difference from the calculated molecular weight (76 kDa) is consistent with the presence of glycosylation. Initial crystallization trials were performed using fully glycosylated sample. Crystals were obtained under the condition 0.1 *M* sodium acetate pH 4.5, 1.2 *M* sodium dihydrogen phosphate at 293 K and grew to dimensions of approximately 30 × 30 × 100 µm within two months (Fig. 2*a*). Processing of the X-ray diffraction images indicated that the unit-cell parameters of the crystal were $a = b = 125.8$, $c = 292.7$ Å (Fig. 2*a*). However, the resolution limit of X-ray diffraction was very low (below 6 Å) and we could not determine the atomic resolution structure using these crystals. We reasoned that the presence of highly flexible glycan chains in the crystal prevented ordered tight packing of the LR11 Vps10p domain. Therefore, we trimmed the glycan

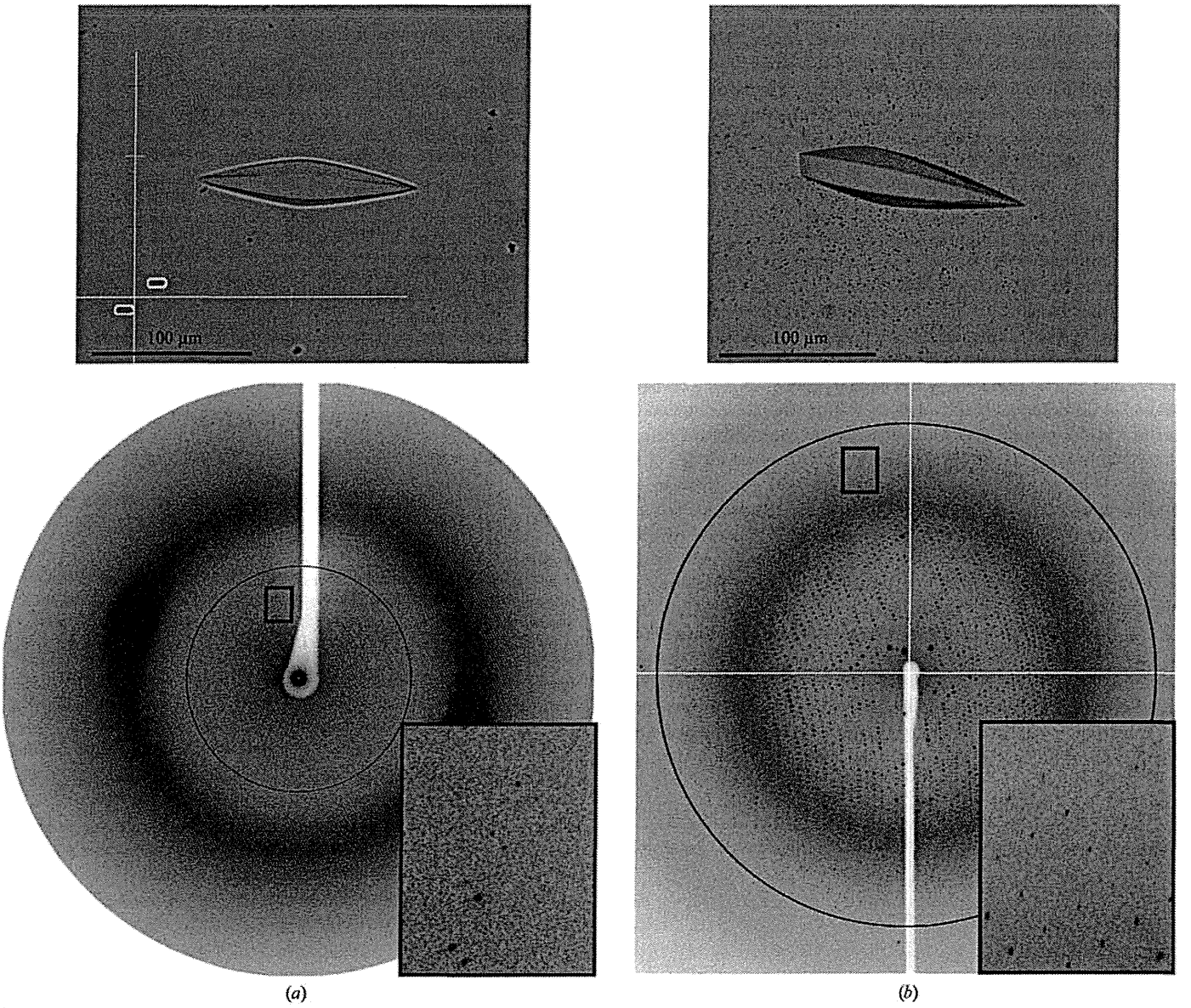

Figure 2
Crystals and diffraction patterns obtained using samples before (*a*) and after (*b*) Endo H treatment. 6.0 Å (*a*) and 2.4 Å (*b*) resolution circles are shown. Expanded views of the regions marked with a rectangle are shown in the insets.

chains from the purified protein using Endo H. Endo H cleaves between the two GlcNAc residues at the base of N-glycans, leaving a single GlcNAc residue at each glycosylation sequon that maintains overall protein solubility. Although Endo H exhibits varying degrees of cleavage efficiency towards different glycan chains, it is able to efficiently cleave the $Man_5GlcNAc_2$ chain, which is the predominant glycoform present on proteins expressed in CHO lec 3.2.8.1 cells (Davis *et al.*, 1993). Endo H treatment of LR11 Vps10p domain resulted in a reduction of the relative molecular mass by ~6 kDa, which is consistent with the complete removal of six glycan chains (Fig. 1). The deglycosylated sample could be crystallized under the same conditions and with the same incubation period (~2 months) as the untreated sample (Fig. 2*b*). Remarkably, the quality of the crystals was dramatically improved and the crystals diffracted to 2.4 Å resolution (Fig. 2*b*), while the unit-cell parameters ($a = b = 126.4$, $c = 290.3$ Å) remained essentially unchanged from the original crystal of fully glycosylated sample (Table 1).

The symmetry and systematic absences of the diffraction intensities indicated that the new crystal of deglycosylated LR11 Vps10p domain belonged to either space group $P6_122$ or its enantiomer $P6_522$. In an attempt to determine the initial phases, the molecular-replacement method was performed using the atomic coordinates of the sortilin Vps10p domain (PDB code 3f6k; Quistgaard *et al.*, 2009) as a search model. Specifically, the β-propeller module was extracted from the coordinates. In addition, residues and atoms that do not map onto the sequence of the LR11 Vps10p domain were deleted from the model with the 'FILE_SEQUENCE' option of *MOLREP*. While the sortilin Vps10p domain shows only 25% sequence identity to the LR11 Vps10p domain, it gave a clear solution in $P6_122$ for which the peak-to-noise ratios of the rotation and translation functions were 5.46 and 24.85, respectively. One monomer was located in the asymmetric unit, showing an R factor of 62.8%. The resulting model was subjected to initial rigid-body and subsequent restrained refinement, which resulted in a reduction of the R and R_{free} factors to 55.5% and 55.9%, respectively. Preliminary model building revealed that all of the potential N-linked glycosylation sites are located on the surface of the protein and we could identify clear electron density that is likely to represent the remaining GlcNAc moiety at five of the six sites. Furthermore, three of these sites are very close to the neighbouring molecules. Although the three N-glycans are not directly involved in crystal packing, it is possible that deglycosylation with Endo H stabilized the packing by lowering the disorder arising from the flexibility of the carbohydrates. In fact, the Matthews coefficient (Matthews, 1968) and solvent content (4.4 $Å^3\,Da^{-1}$ and 72.2%, respectively) suggested a loose crystal packing (Kantardjieff & Rupp, 2003), indicating the presence of a large space that can accommodate flexible N-glycans. Further model building and structure refinement are now in progress and the mechanism by which the deglycosylation improved the crystal quality may be clarified after completion of the model assignment, including the carbohydrates.

We would like to thank Drs L. M. G. Chavas, Y. Yamada, N. Matsugaki and N. Igarashi of the Photon Factory and E. Yamashita, M. Suzuki and A. Nakagawa of SPring-8 BL44-XU for providing data-collection facilities and for support. We also thank K. Tamura-Kawakami, E. Mihara and M. Nampo for their excellent technical support and M. Nakano for preparation of the manuscript. This work was partly supported by a Grant-in-Aid for Scientific Research (A) from the Ministry of Education, Culture, Sports, Science and Technology of Japan (MEXT), by a Grant-in-Aid for Scientific Research on Priority Areas from MEXT and by a Protein 3000 Project grant from MEXT.

References

Andersen, O. M. *et al.* (2005). *Proc. Natl Acad. Sci. USA*, **102**, 13461–13466.
Andersen, O. M., Schmidt, V., Spoelgen, R., Gliemann, J., Behlke, J., Galatis, D., McKinstry, W. J., Parker, M. W., Masters, C. L., Hyman, B. T., Cappai, R. & Willnow, T. E. (2006). *Biochemistry*, **45**, 2618–2628.
Bettens, K., Brouwers, N., Engelborghs, S., De Deyn, P. P., Van Broeckhoven, C. & Sleegers, K. (2008). *Hum. Mutat.* **29**, 769–770.
Bork, P., Downing, A. K., Kieffer, B. & Campbell, I. D. (1996). *Q. Rev. Biophys.* **29**, 119–167.
Chen, Z.-Y., Ieraci, A., Teng, H., Dall, H., Meng, C.-X., Herrera, D. G., Nykjaer, A., Hempstead, B. L. & Lee, F. S. (2005). *J. Neurosci.* **25**, 6156–6166.
Davis, S. J., Puklavec, M. J., Ashford, D. A., Harlos, K., Jones, E. Y., Stuart, D. I. & Williams, A. F. (1993). *Protein Eng.* **6**, 229–232.
Emsley, P. & Cowtan, K. (2004). *Acta Cryst.* D**60**, 2126–2132.
Hermans-Borgmeyer, I., Hampe, W., Schinke, B., Methner, A., Nykjaer, A., Süsens, U., Fenger, U., Herbarth, B. & Schaller, H. C. (1998). *Mech. Dev.* **70**, 65–76.
Kantardjieff, K. A. & Rupp, B. (2003). *Protein Sci.* **12**, 1865–1871.
Lee, J. H., Cheng, R., Schupf, N., Manly, J., Lantigua, R., Stern, Y., Rogaeva, E., Wakutani, Y., Farrer, L., St George-Hyslop, P. & Mayeux, R. (2007). *Arch. Neurol.* **64**, 501–506.
Marcusson, E. G., Horazdovsky, B. F., Cereghino, J. L., Gharakhanian, E. & Emr, S. D. (1994). *Cell*, **77**, 579–586.
Matthews, B. W. (1968). *J. Mol. Biol.* **33**, 491–497.
Motoi, Y., Aizawa, T., Haga, S., Nakamura, S., Namba, Y. & Ikeda, K. (1999). *Brain Res.* **833**, 209–215.
Murshudov, G. N., Vagin, A. A. & Dodson, E. J. (1997). *Acta Cryst.* D**53**, 240–255.
Nogi, T., Yasui, N., Hattori, M., Iwasaki, K. & Takagi, J. (2006). *EMBO J.* **25**, 3675–3683.
Offe, K., Dodson, S. E., Shoemaker, J. T., Fritz, J. J., Gearing, M., Levey, A. I. & Lah, J. J. (2006). *J. Neurosci.* **26**, 1596–1603.
Ohwaki, K., Bujo, H., Jiang, M., Yamazaki, H., Schneider, W. J. & Saito, Y. (2007). *Arterioscler. Thromb. Vasc. Biol.* **27**, 1050–1056.
Otwinowski, Z. & Minor, W. (1997). *Methods Enzymol.* **276**, 307–326.
Quistgaard, E. M., Madsen, P., Groftehauge, M. K., Nissen, P., Petersen, C. M. & Thirup, S. S. (2009). *Nature Struct. Mol. Biol.* **16**, 96–98.
Rogaeva, E. *et al.* (2007). *Nature Genet.* **39**, 168–177.
Scherzer, C. R., Offe, K., Gearing, M., Rees, H. D., Fang, G., Heilman, C. J., Schaller, C., Bujo, H., Levey, A. I. & Lah, J. J. (2004). *Arch. Neurol.* **61**, 1200–1205.
Spoelgen, R., von Arnim, C. A., Thomas, A. V., Peltan, I. D., Koker, M., Deng, A., Irizarry, M. C., Andersen, O. M., Willnow, T. E. & Hyman, B. T. (2006). *J. Neurosci.* **26**, 418–428.
Stanley, P. (1989). *Mol. Cell. Biol.* **9**, 377–383.
Vagin, A. & Teplyakov, A. (2010). *Acta Cryst.* D**66**, 22–25.
Willnow, T. E., Petersen, C. M. & Nykjaer, A. (2008). *Nature Rev. Neurosci.* **9**, 899–909.
Yamazaki, H., Bujo, H., Kusunoki, J., Seimiya, K., Kanaki, T., Morisaki, N., Schneider, W. J. & Saito, Y. (1996). *J. Biol. Chem.* **271**, 24761–24768.

Atherosclerosis 210 (2010) 581–584

Contents lists available at ScienceDirect

Atherosclerosis

journal homepage: www.elsevier.com/locate/atherosclerosis

Enhanced circulating soluble LR11 in patients with coronary organic stenosis

Mao Takahashi[a], Hideaki Bujo[b], Meizi Jiang[b], Hirofumi Noike[a], Yasushi Saito[c], Kohji Shirai[d,*]

[a] Department of Cardiovascular Center, Sakura Hospital, Medical Center, Toho University, Chiba, Japan
[b] Department of Genome Research and Clinical Application, Chiba University Graduate School of Medicine, Chiba, Japan
[c] Department of Clinical Cell Biology, Chiba University Graduate School of Medicine, Chiba, Japan
[d] Department of Internal Medicine, Sakura Hospital, Medical Center, Toho University Sakura, Japan

ARTICLE INFO

Article history:
Received 3 April 2009
Received in revised form
27 November 2009
Accepted 7 December 2009
Available online 16 December 2009

Keywords:
LR11
Coronary stenosis
Hyperglycemia
Intimal smooth muscle cell

ABSTRACT

LR11, an LDL receptor family member, is expressed in intimal smooth muscle cells. It was found that the soluble form of LR11 (sLR11) is detected in serum, and the circulating sLR11 levels are positively correlated with intima-media thickness of carotid arteries in dyslipidemic subjects. To clarify the significance of serum sLR11, the circulating sLR11 levels in patients with organic coronary stenosis and the contributing risk factors for them were studied. The subjects, 150 patients with symptoms of coronary artery disease, underwent coronary angiographic examination, and were divided into sex- and age-matched two groups; one is organic coronary stenosis group (OCS) and the other is normal coronary group (NC). Serum sLR11 levels were significantly higher in OCS than in NC (4.9 ± 2.7 U vs 3.6 ± 1.8 U, $p < 0.05$). Multivariate regression analysis showed that circulating sLR11 is independent contributing factor for the OCS, as well as diabetes mellitus and dyslipidemia. Among various coronary risk factors for sLR11 level, HbA1c showed the highest correlation coefficient ($p < 0.01$).

These results suggest that the circulating sLR11 might reflect coronary organic stenosis, and that hyperglycemic condition might be promoting factor for expression of LR11 in intimal smooth muscle cells.

1. Introduction

In the formation of atherosclerosis, migration of vascular smooth muscle cells (SMCs) from the media to the intima is the key step [1,2]. Following migration, SMCs change the phenotype and proliferate in the intima, resulting in intimal thickness. Furthermore, proliferating SMCs secrete matrices and proteases to form atheromatous lesions under the influence of stimulatory cytokines [3–6].

Recently, we [7] identified LR11, which is an LDL receptor family member with poorly defined function, and observed the expressing of LR11 specifically in intimal SMCs, but not in medial SMCs, macrophages or lymphocytes in the arterial wall [7–10]. LR11 as both the membrane-spanning and the shed soluble (sLR11) forms bind to urokinase-type plasminogen activator receptor (uPAR) on the cell surface [8,11]. Over-expression of LR11 in SMCs enhances their migration via elevated levels of uPAR, and appears to thereby increase the activation of the uPA system [7,12].

Interestingly, the sLR11 was detected in the serum, and that the circulating sLR11 levels are positively correlated with intima-media thickness of carotid arteries in dyslipidemic subjects [13]. The relationship of the sLR11 levels in serum with other risk factors for atherosclerosis, such as age, sex, smoking, blood pressures, serum lipids, and plasma glucose was not observed. But, the precise was not clear yet.

It is reported that arterial intimal thickening after balloon catheter injury was enhanced in diabetic animals than control [6,14]. Clinically, increased intimal-medial thickness of carotid artery in type 2 diabetes was reported [15,16]. Thus, a relationship between coronary stenosis and sLR11 level, and also a relationship between sLR11 and diabetic condition were suspected.

In this report, we investigated the significance of circulating sLR11 in organic coronary stenosis (OCS) of the patients with a suspicion of coronary artery diseases (CAD). Contributing factors for the elevation of serum sLR11 were also analyzed.

2. Subject and methods

The subjects were 150 persons who were suspected to have coronary artery disease and who underwent coronary angiography at Toho University Sakura Hospital Cardiovascular Center were

* Corresponding author at: Department of Cardiovascular Center, Toho University School of Medicine Sakura Hospital, Sakura 285-8741, Japan.
E-mail address: kshirai@kb3.so-net.ne.jp (K. Shirai).

0021-9150/$ – see front matter © 2009 Elsevier Ireland Ltd. All rights reserved.
doi:10.1016/j.atherosclerosis.2009.12.010

recruited for the study. Patients suffered from chronic heart disease with ejection fraction < 50% or chronic renal failure with serum creatinine >1.3 mg/dl were excluded from the study analysis. The study protocol was approved by the Human Investigation Review Committee of Toho University Sakura Hospital, and informed consent was given by each patient.

The angiographical severity of coronary stenosis was assessed in the worst view position, and the percentage of luminal narrowing was recorded according to the American Heart Association reporting system [17]: organic coronary stenosis was defined as a stenosis with ≥75% diameter, and normal coronary artery (NC) was defined as without significant stenosis. Blood sample were collected in the morning after an overnight fast. Lipid variables and fasting blood glucose were measured by standard laboratory techniques. Serum insulin was measured by an enzymatic-immunological assay. Homeostasis model assessment insulin resistance index (HOMA-IR) was defined as: (plasma glucose × serum insulin)/405 [18]. Potential risk factors for atherosclerosis were analyzed, including age, sex, body mass index (BMI), smoking, and histories of hypertension, diabetes mellitus or dyslipidemia. Hypertension was defined as a history of hypertension (systolic pressure > 140 mmHg or diastolic pressure >90 mmHg). Diabetes mellitus was defined as a history of diabetes mellitus having fasting blood glucose >126 mg/dl and HbA1c >5.8%. Dyslipidemia was defined as a history of serum total cholesterol >220 mg/dl and/or triglyceride >150 mg/dl in the fasting and/or HDL-cholesterol <40 mg/dl.

3. Measurement of serum sLR11 concentration

Fasting blood samples were collected and were centrifuged immediately after collection to measure serum sLR11 levels. Fifty microliters of serum was purified using a 39 kDa receptor-associated protein (RAP)-GST affinity beads (Cosmo Bio). For immunoblotting, equal amount of protein extracted from pelleted beads was subjected to 10% SDS-PAGE after heating to 95 °C for 5 min as described [13] under reducing conditions, and transferred to a nylon membrane. Incubations were with antibody against LR11 (5-4-30-19-2 at 1:500 dilution) [13], followed by peroxidase-conjugated anti-mouse IgG. Development was performed with the ECL detection reagents (Amersham Pharmacia). The signals were quantified by densitometric scanning using NIH image™ software. The sLR11 levels in each human serum (50 μl) was determined as an averaged value of three quantified signal intensities resulting from independent assays using samples with blind indication, and expressed as a ratio to that of a standard serum. The immunological estimation indicated that the signal of 1 U (in 50 μl serum) corresponded to approximately 50 ng/ml of recombinant sLR11.

4. Statistics

The results are shown as mean ± SD or proportion (%) for each index. Statistical analysis was performed with SPSS version 13.0 (SPSS Japan Inc.). The unpaired *t*-test and the *chi*-square test were used to compare the continuous and the categorized variables, respectively. Pearson's correlation coefficient analysis was used to assess association between measured parameters. Subsequently, multiple linear regression analyses were used to calculate the ORs for the OCS (i) by controlling for all risk factors (age, sex, BMI, smoking, diabetes, hypertension, dyslipidemia and sLR11) (Model 1); (ii) by additionally controlling for BMI, diabetes, dyslipidemia, and sLR11, which are significantly associated with OCS by above analyses (Model 2). These risk factors were scored as explanatory factors, and subordinate variable was OCS = 1 and NC = 0. A value of $p < 0.05$ was considered significant. Multivariate analysis was performed by multiple regression analysis.

Table 1
Characteristics of the normal coronary artery and organic coronary stenosis subjects.

	NC	OCS	*p* value
n	55	95	
Male (%)	65.5	74.7	0.23
Age (y)	66.1 ± 8.4	66.5 ± 9.7	0.87
BMI (kg/m^2)	23.9 ± 3.0	25.1 ± 3.4	<0.05
Diabetes (%)	5.5	33.7	<0.01
Hypertension (%)	56.4	64.2	0.34
Dyslipidemia (%)	52.7	85.3	<0.01
sLR11(U)	3.6 ± 1.8	4.9 ± 2.7	<0.01
Fasting blood sugar (mg/dl)	106.7 ± 13.4	111.5 ± 27.1	0.22
Insulin (μU/dl)	6.2 ± 3.9	7.9 ± 4.9	<0.05
HOMA-IR	1.7 ± 1.1	2.2 ± 1.9	<0.05
Medications			
Administration of statin (%)	18.2	66.3	<0.01
Administration of ACE-I or ARB (%)	29.1	42.1	0.13

Plus–minus values are means ± SD. The unpaired *t*-test was used for continuous variables, and the *chi*-square test was used for categorized variables. BMI: Body mass index. Circulating sLR11 levels in NC group and OCS group were 3.6 ± 1.8 U and 4.9 ± 2.7 U, respectively, indicating that the sLR11 levels in OCS were significantly higher than those in NC ($p < 0.01$).

5. Results

5.1. Circulating sLR11 levels in NCA and OCS groups

The subjects were classified into age- and sex-matched two groups, according to the angiographical evaluation. Normal coronary artery group is composed of 55 subjects and organic coronary stenosis group is composed of 95 subjects (Table 1). BMI, histories of diabetes and dyslipidemia were significantly increased in the OCS group comparing with the NC group. Smoking and the history of hypertension were not different between the two groups. Insulin levels and HOMA-IR levels were significantly increased in the OCS group. Circulating sLR11 levels in NC group and OCS group were 3.6 ± 1.8 U and 4.9 ± 2.7 U, respectively, indicating that the sLR11 levels in OCS were significantly higher than those in NC ($p < 0.01$). Note that we have reported that the mean circulating sLR11 levels in four-hundreds dyslipidemic subjects are 3.0 ± 1.0 U [13]. Thus, circulating sLR11 levels increased in the patients with organic coronary stenosis among the patients taking angiographical examination with a suspicion of coronary arterial diseases.

5.2. Multivariate analysis of sLR11 and other risk factors for OCS

We next analyzed the significance of sLR11 in comparison to other risk factors for OCS in all subjects (Table 2). The multivariate analysis of all variables (Model 1) for OCS showed that circulating sLR11 and the histories of diabetes or dyslipidemia were explanatory factor for OCS independent from other variables. The Model 2 analysis using the limited variables which have been shown to be significantly increased in OCS (see Table 1) showed that circulating sLR11 is still an independent factor for OCS. These results showed that the circulating sLR11 level was enhanced in OCS group among patients with a suspicion of CAD and taking coronary angiography.

5.3. Correlation of serum sLR11 with other various parameters in all subjects

As shown in Table 3, a negative correlation between sLR11 concentration and HDL-cholesterol ($r = -0.161$, $p < 0.05$) and a positive correlation between sLR11 and triglyceride ($r = -0.161$, $p < 0.05$) were found. Furthermore, BMI ($r = 0.182$, $p < 0.05$), insulin (0.186, $p < 0.05$) and HOMA-IR (0.242, $p < 0.01$) and HbA1c ($r = 0.272$, $p < 0.01$) showed significant positive correlations with sLR11, respectively. But there was no significant correlation between cir-